Pure & Appl. Chem., Vol. 60, No. 8, pp. 1175–1183, 1988.
Printed in Great Britain.

Chemical characterization and X-ray absorption spectroscopy

H.L. Nigam

Chemical Laboratories, A.P.S.University,Rewa(M.P.)-486003,India

Abstract:- A rapid progress in the theoretical developments based on modulations of absorption cross section due to single and multiple scattering of an electron emitted from an inner shell by X-rays impinging on the target atom to understand the EXAFS and XANES in recent years and harnessing of the highly powerful synchrotron radiation source for the X-rays have bestowed immense capability on X-ray absorption spectroscopy for elucidation of chemical structure. Some spectacular advances made have been discussed with illustrative examples.

INTRODUCTION

X-ray absorption spectroscopy has, in recent years, assumed an important role as a technique of structure determination(ref.1). A decided advantage of this technique lies in its structural application to complex biological or chemical systems, polymeric or amorphous solid, liquid or gas where single crystals are not available and other conventional methods fail to give unambiguous results. Infact, in the beginning of the century, X-ray spectroscopy first provided the experimental basis of the quantum theory of atoms leading to basic information on the electronic structure of atoms but in absence of intense continuum radiation sources, this spectroscopy after the first quarter did not make much headway. The sudden boost and credibility that the technique has recieved durimg the last decade is due to harnessing of the highly powerful synchrotron radiation source for X-rays where source brightness would give tuneable X-rays of intensity greater by several orders of magnitude than the X-rays obtained from any conventional source making it possible to probe the extremely metal-dilute systems like metalloenzymes and also enabling extremely rapid data collection (ref. 2,3). Also a clear discerning of the theory of the Extended X-ray Absorption Fine Structure (EXAFS) by Sayers, Stern and Lytle (ref.4) and rapid theoretical progress on EXAFS (ref.5,6,7) combined with development of a sound theoretical base for X-ray Absorption Near Edge Structure(XANES) (ref.8.9.10) have enormously enhanced the scope of obtainable information regarding local structure that plays a key role on the properties of complex systems such as the biological functions of proteins, chemisorption of molecules on surfaces, electronic properties of amorphous materials and catalyst activities.

THE X-RAY ABSORPTION SPECTRUM

The intensity of X-ray beam is attenuated by passing through the sample leading to X-ray absorption spectroscopy. The absorption jumps, "edges" characteristic of each element in the sample arise where the incident photon has just sufficient energy to promote a core electron to unoccupied valence levels or to the continuum, thus, k-edge arises from 1s excitation, L-edge arise from 2s or 2p excitation and so on (ref.11). The X-ray absorption spectrum is characteri -sed by a steeply rising energy vs. absorption coefficient (logIo/It) arc tangent shaped curve, called the absorption edge followed by a train of dampening fluctuations in the intensity to the high energy side, running over several hundred electron volts beyond the main edge (Fig.1a,b). The electronic transitions are decided by a number of considerations including the symmetry and overlap of wave functions and the covalent mixing parameters in occupied and unoccupied orbitals. The spectra may be considered in four parts(Fig.2):

i) the pre-edge structure,
ii) the absorption edge,
iii) the structure near the absorption edge (50eV) called XANES,and
iv) the structure beyond 50eV called EXAFS.

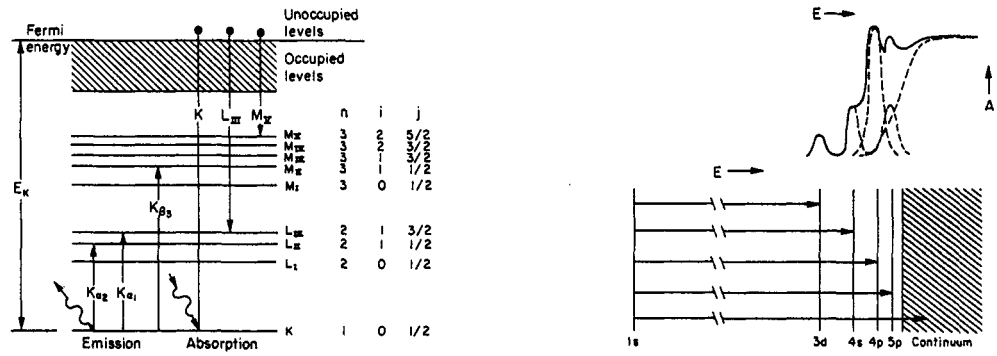

Fig. 1. Schematic diagrams of (a) emission and absorption processes and (b) X-ray absorption edge showing relation between bound state transition and observed spectrum (ref.11).

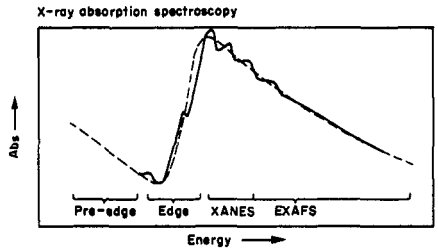

Fig. 2. Schematic representation of a typical X-ray absorption spectrum (ref.11).

THE PRE-EDGE REGION

The assignment of electronic transitions to structures appearing in this region is basic to the assignment of bonding orbitals in the complex. In case of transition metal complexes having vacant low lying energy d-orbitals such an assignment is straightforward, namely 1s-> nd (quadrupules transition $\Delta l=+2$), a feature that may appear and be enhanced in intensity as a result of mixing of d,s,p character in the orbitals (produced for example by covalent mixing and or tetrahedral symmetry). Thus, the absence of this feature on the Mo K-edge in Mo-Fe protein, clostridium , pasteurianum as against the enhancement of 1s->4d transition on the spectra of thiomolybdates, has recently led Cramer et al (ref.12) to eliminate tetrahedral geometry in the former (Fig.3). In case of cobalt thiopropionic acid complexes, we have observed two small maxima in 1s-->3d region attributable to the splitting of the 3d orbitals into 3d(t_{2g}) and 3d(eg) under the influence of crystal field; the energy separation being nearly the same as 10Dq value reported for the complex (ref.13).

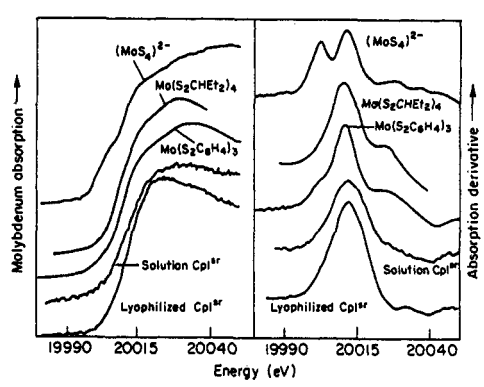

Fig. 3.X-ray absorption spectra showing a comparison of lyophilized and solution clostridium pasteurianum (semi-reduced) with three molybdenum compounds with all sulphur coordination.

THE ABSORPTION EDGE

The shape of the absorption edge which is determined by relative intensities and width of low lying bound state transitions contain information about the geometry of the metal complex and nature of the ligands present. The

position of the absorption edge features are sensitive to the metal oxidation state and environment. According to molecular orbital approach, the X-ray absorption edge features correspond to electronic transitions to successive molecular orbitals (of the complex) having primarily metal character.

EXAFS

Although the bound state transitions could account for most of the structure within 25eV of the absorption edge, the theory did not give any satisfactory explanation for additional structures which are invariably observed, for part of XANES (i.e. the low energy Kosseel structure probing the empty electronic states) and entire EXAFS (i.e. high energy Kronig structure probing the local structures). The raging controversy between, "long range order theories" formulated in terms of Block wave for the excited photoelectron final state and "short range order theories" including/involving photoelectron scattering by neighbouring atoms in case of Kronig structure were extensively studied by a number of pioneers (Kronig 1931, Peterson 1936, Kostarev 1941, Hayashi 1949, Savada 1958, Kozlenkov 1961, Azaroff 1963, Lytle 1964, Levy 1965, Obashi 1967) but the breakthrough came with the work of Sayers et al (ref. 4) who showed that a single scattering "short range order theory", through proper interpretation of the phase, amplitude and frequency of the EXAFS oscillation can provide information about type, number and distance of atoms in the vicinity of the absorber (also ref. 14, 15).

The theory has been placed on firm foundation by the work of Ashley and Doniach (1975) (ref. 5) and Lee and Pendry (1975) (ref. 6). The new approach may be understood by considering that on absorption of an X-ray photon by an electron in the K-shell of a particular atom, the electron gets ejected. This is equivalent to spherical waves radiating from atom into the surrounding matter. Whenever the wave encounters other atoms, it will partially be reflected and will interfere with the outgoing wave. The net interference pattern at the nucleus of the initially absorbing atom will then modify the crosssection of the initial absorption process (Fig. 4).

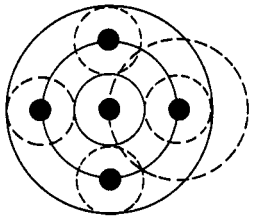

Fig. 4. The scattering processes that occur in EXAFS. Shaded circles represent the position of the atoms in the condensed state. The plane wave emanates from the central atom. Solid circles represent the crests of the outgoing part of the wave, which after diffraction by the surrounding atoms is indicated by the dashed circles.

The fine structure extending to several hundred volts higher in energy is produced by the progressively shortening wave-length of the spherical wave yielding additional nodes in the pattern. Sayers et al. showed that the effects can be theoretically unravelled from the Fourier transformation of the EXAFS spectrum. Thus, the EXAFS (K) is defined as the modulation of absorbing coefficient on the high energy side and can be given the expression:

$$\chi(K) = \frac{\mu - \mu_s}{\mu_0} \cong \frac{1}{K} \sum N_S \frac{|f_s(\pi, K)|}{R_{as}^2} \exp(-2\sigma_{as}^2 K^2) \sin[2K R_{as} + \alpha_{as}(K)]$$

where μ_0 is the absorption coefficient in the absence of neighbouring atoms, μ_s is the observed absorption, k is the photoelectron wave vector, N_S is the number of scatterers (S) at a distance R_{as} from the absorber (a), $f_s(\pi,k)$ is the scatterers electron back scattering amplitude, α_s is the total phase-shift and σ_{as}^2 is the mean suqare deviation of R_{as}. Thus, the frequency of oscillations is proportional to the distance between the absorber and the scatterers (i.e. the central metal atom and neighbouring ligands in a complex), the phase-shift $\alpha_{as}(K)$ due to electron atom back-scattering and propagation out of and back through the coulomb hole affecting both the frequency and the absolute phase of EXAFS. Also, the EXAFS amplitude will be proportional directly to the number of scatterers weighted by their electron atom back scattering amplitude $f_s(\pi,k)$ and damped by an inverse square dependence on fluctuations of $R_{as}(-\sigma_{as}^2 K^2)$ (ref.11). The summation index is overall scattering atoms in the vicinity of the absorber. The variable k is the photoelectron wave vector which is related to the photon energy E by the expression :

$$K = \left[\frac{2m}{\hbar^2}(E - E_0)\right]^{1/2}$$

where E_o is the energy threshold for an electron ejected from the absorbing atom. The use of Fourier transformation to analyse EXAFS was introduced by Sayers, Lytle and Stern. They showed that the major peaks in the transform correspond to important absorber-scatterer distance but shifted to a lower R by a few tenths of an Angstrom. The transform peak height is related to the magnitude of a particular frequency component while peak position is related to half the average frequency of the component. The effective phase-shift (peak position- true distance) and effective per atom magnitude (peak height multiplied by square of the distance divided by scatter number) have to be obtained from analysis of model compounds and then the transform peak position and height can be used to predict scatterer distances which on being used for curve fitting analysis give final conclusion. An excellent illustration is provided bythe work of Cramer et al. (ref.12) on nitrogenase, where the smooth shape and low energy position of the absorption edge show primarily sulphur ligation(Fig.3) and the final conclusion streaming from the three shall fit (Fig.5) are that Mo in lyophilised clostridium pasteourianum in the semi-reduced state is surrounded by three or four sulphurs at 2.35 ± 0.3Å (nearer Mo-S bridging bond length), one or two sulphurs at 2.49± 0.03Å (nearer Mo-S cystine terminal bond length), two or three irons at 2.72+ 0.05Å (nearer sulphido-bridged iron bond length).

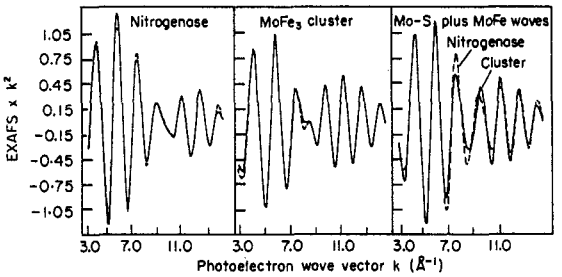

Fig. 5. Curve-fitting analysis of nitrogenase and th Mo-Fe cluster compound fitted with three-waves including Mo-S wave.

On this clue Holm and coworkers (ref.16) have succeeded in synthesising a Mo-Fe-S cluster.[$Fe_6Mo_2S_9$ $(SEt)_8]^{3-}$ the crystal structure of which is shown in (Fig.6)The EXAFS of the compound is almost similar to that of nitrogenase molybdenum.

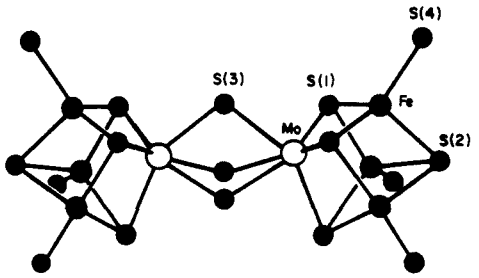

Fig. 6. Arrangement of central atoms of [$Fe_6Mo_2S_9(SEt)_8$]$^{3-}$

BOND-ANGLE DETERMINATION FROM EXAFS

The EXAFS formalism based on single scattering suffers from a serious limitation that the distance determination can be made only upto about 4Å. It fails in situations where there is a "focussing" effect of the amplitude due to neighbouring atoms and the absorbing atom being arranged in a colinear fashion. In this case multiple scattering processes the intervening atoms must be considered. The single scattering formalism of EXAFS also does not give any information about the bond-angle except that in some cases such an information can be extracted by polarisation dependent measurement on single crystals.

Recently Teo(ref.17,18) has developed a new EXAFS formulation which takes into account the effect of multiple scattering. He has given a method based on multiple scattering for determination of inter-atomic angle by EXAFS. This marks a major advance in the theory of EXAFS and it has been possible to calculate theoretical scattering amplitude and phase functions for various scattering angles. The method is applicable to systems with bond-angles greater than ~100°.

Teo has shown that in a three-atom system ABC where A is the X-ray absorbing atom(central atom), B is the nearest neighbour and C is the next nearest

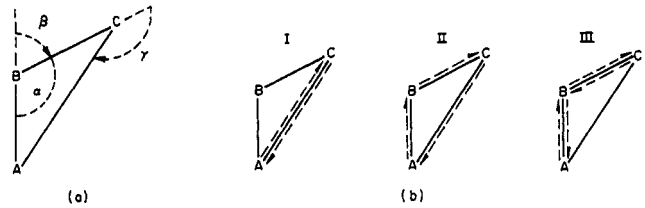

Fig. 7. Schematic representation of a three-atom ABC system and representation of the three scattering pathways (ref.18).

neighbour (Fig.7), with α as the bond angle ABC and β and γ as scattering angles at atoms B and C; the EXAFS of the absorber A would comprise of two contributions one from the back scattering of B(designated as AB) and the other from the back scattering of C via the intermediary atom B(designated as AC) and the three pathways would be: (Fig. 7b)

i) direct back scattering from A to C and back (viz. A-->C-->A),
ii) multiple scattering via atom B (viz. A-->B-->C-->A or A-->C-->B-->A), and
iii) multiple scattering again via intervening atom B (viz.A-->B-->C-->B-->A).

The EXAFS for an unoriented sample corresponding to the AC distance is then the sum of three terms representing these pathways, which can be simplified to:

$$\chi^{ABC}(K) = \frac{1}{K r_{AC}^2} \Omega_B(\beta, K)\, F_C(K)\, e^{-2\sigma_{AC}^2 K^2} e^{-2 r_{AC}/\lambda}$$

$$\sin\left[2K r_{AC} + \phi_{AC}(K) + \omega_B(\beta, K)\right]$$

Here both $\Omega_B(\beta,K)$ and $\omega_B(\beta,K)$ are functions of the scattering angle β. Thus, by substituting the modified amplitude $F_C(K)\,\Omega_B(\beta,K)$ for $F_C(K)$ and the corrected phase $\phi_C(K) + \omega_B(\beta,K)$ for $\phi_C(K)$, the EXAFS data can be analysed in the usual way. This equation can be conversely used to determine β and the bond angle α is given by $180-\beta$.

XANES

As said earlier, the X-ray absorption near edge structure was assigned to the "partial local density of states" of the conduction band. The detailed calculations including high energy empty levels and final state effects as excitons and many body effects made it insurmountably difficult to proceed beyond the first 8 eV in metals and insulators. Molecular orbitals approach was invoked to explain, with only limited success the final states as calculated empty valence orbitals in the complexes. In the new approach scattering of the electron emitted froman inner shell modulates the absorption cross-section. At low electron energies absorption cross-sections are high and strong modulations in the cross section results (Fig. 8) (ref.19)

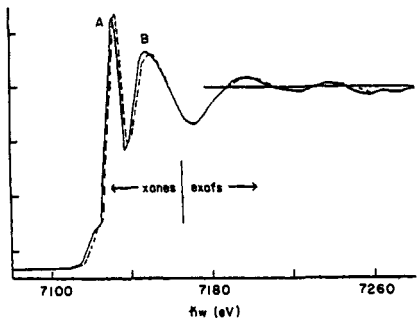

Fig. 8. The relative absorption coefficient for X-rays in the vicinity of the iron K-edge shown for $K_4Fe^{II}(CN)_6.3H_2O$ (————) and $K_3Fe^{III}(CN)_6$ (-----) (ref.19)

At higher energies weaker modulations occur as a result of weaker scattering which is the domain of EXAFS. In the XANES domain, the photoelectron is strongly back scattered generating a multiple scattering process. Bianconi and coworkers have assigned the XANES peaks extending from 8eV to 40eV above the threshold as multiple scattering resonances of the excited photoelectron scattered by neighbour atoms in continuum part of the spectrum

in their investigations extending from simple systems to complex biological molecules and surfaces (ref.20,21,22). Taking a clue that in the independent particle model the electron states are calculated from a 1-electron Schrodinger equation containing an effective potential function, Durham(ref.23) has shown that if the potential around the X-ray excited atom is represented by a finite cluster of non-overlapping muffin-tin potentials each of whose scattering power is given by a t matrix for angular momentum $L \equiv (l,m)$, the rate at which the system absorbs X-rays of energy $\omega(\hbar=1)$ by excitation from a core state C can be written as :

$$W_c(\omega) = -2 \sum_{LL'} m_L^i(\varepsilon)\, \mathrm{Im}\, \tau_{LL'}^{ii}(\varepsilon)\, m_{L'}^{i*}(\varepsilon)\, \theta(\varepsilon-\mu)$$

where ($\varepsilon = \varepsilon_c + \omega$) and $m_L^i(\varepsilon)$ is an atomic-like dipole matrix element linking the core state with high energy states (with angular momentum L) of the single muffin-tin potentials at the excited atom (here given a site index i). The scattering path matrix $\tau_{LL'}^{ii}$ summarises the multiple scattering paths relevant to X-ray spectra. Thus, he gave a general result for any array of non-overlapping scatterers as :

$$\sum_{K,L''} (t_{i,L}^{-1}\, \delta_{iK}\, \delta_{LL''} - g_{LL''}^{iK})\, \tau_{L''L'}^{KJ} = \delta_{iJ}\, \delta_{LL'}$$

where $g_{LL''}^{iK}$ describes the propagation of the free spherical wave from site i to site k. This result entails matrix inversion which is not so easy a task.

An excellent example of the use of XANES theory is provided by the study of local geometry variation between the $[Fe^{II}(CN)_6]^{4-}$ and $[Fe^{III}(CN)_6]^{3-}$ clusters. The EXAFS gives very nearly the same distances for Fe-C bond for both the oxidation states but a very subtle structural change is expected to occur because of the effect of electron back donation between Fe and CN groups. The XANES show strong oscillations with an approximately 1eV relative shift of the edge to lower energy in the ferrocyanide complex (Fig.9).

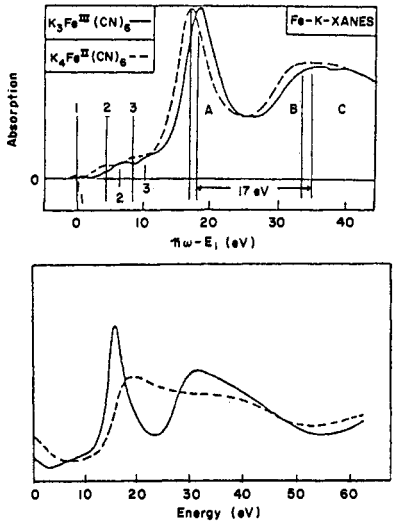

Fig. 9. Iron K-edge XANES of iron hexacyanide complexes $[Fe(CN)_6]^{4-}$ and $[Fe(CN)_6]^{3-}$. The important role of the second neighbour shell is shown by XANES calculations in the lower panel for cluster $[Fe(CN)_6]^{3-}$ with both C and N shells included (full curves) and with the C first shell only included(dashed curve). The energy shift of peak A follows the Fe-C distance variation, the shape and intensity ratio between peaks A, B and C follow the geometric distortions induced by different charge state of the cluster.(ref.24)

Besides the shift of peak A in Fig.9 a change of shape of the features B and C is also observed. Bianconi(ref.24) has shown that a contraction of the Fe-C distance induces an increase of A-B energy splitting in the XANES. Distortions in geometry induce changes in the shapes of B and C as well as of peak A. Thus different XANES spectra indicate the subtle structural differences like different C-N distances and distortions of octahedral symmetry induced by an extra electronic change on $Fe(CN)_6$ cluster not detected by EXAFS. They also measured and calculated the K XANES of iron in the heme-proteins like haemoglobin and mioglobin (ref.25). A good agreement between theory and experiment was obtained by including nearly 30 atoms in the cluster for XANES calculations. Bianconi and coworkers have also studied the XANES of calcium binding proteins like calmodulin (ref.24) and tropinin-C(ref.24) (Fig.10). It is seen that calcium XANES are affected by binding of Mg^{2+} in some low affinity sites perhaps on the external part of the protein. This is perhaps the only method that gives direct information to the local structure change induced by magnesium.

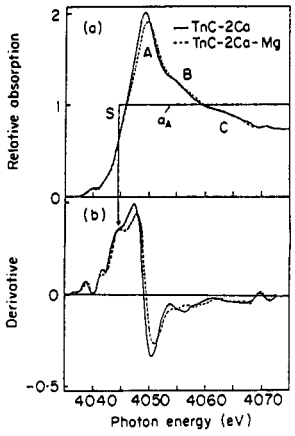

Fig. 10. The XANES spectra of calcium in the calcium binding protein troponin-C. The multiple scattering resonances A,B and C show energy shift and intensity variation due to change in the local geometry (movement of CO and COO^- molecular groups bound to calcium) induced by binding of Mg external low affinity sites of the protein (ref.24).

BOND LENGTH FROM XANES STUDIES

The work of Bianconi, Dell'Ariccia, Gargano and Natoli has given a new dimension to the multiple scattering resonance approach to study XANES. According to them(ref.26) the multiple scattering theory approach to calculations to absorption cross section requires that at a resonance defined as a maximum of the absorption, the determinant of the multiple scattering matrix in the K-matrix asymptotic normalisation:

$$M^{JJ'}_{LL'} = K^{\alpha J}_{LL'}(x)\,\delta_{JJ'} - G^{oJJ'}_{LL'}(x\vec{R}_{ij})$$

must vanish. The vanishing of Det M at a resonance defines an implicit relation of the type $\mathcal{F}[x_r R_{ij}, \delta^J_\ell(x_r)] = 0$

between the reduced wave vector of the resonance $x_r = [E_r - \bar{V}]^{1/2}$

and the distance $\vec{R}_{ij} = \vec{R}_i - \vec{R}_j$ of the various atomic scatterers in the cluster with phase-shift $\delta^J_\ell(x)$. Here E is the photoelectron energy h .I measured from ionisation threshold and V is some sort of muffin-tin constant potential satisfying the condition:

$$\int_r^{r'} [E - V(r(t))]^{1/2}\,\dot{r}(t)\,dt \sim [E-\bar{V}]^{1/2}(r-r')$$

SOME APPLICATIONS

The use of EXAFS and XANES on some typical systems shall now be discussed.

1. A very useful illustration is found in the X-ray absorption spectra of Ru L-edges in $Ru(NH_3)_6Cl_3$ (ref.27), recorded in transmission mode with the EXAFS spectrometer at SSRL using Si(111) crystals. A broad L_I edge as observed as against narrow and intense peaks in the near edge region in L_{II} and L_{III} spectrum; the most striking feature being two sharp resonances A and B exhibited by L_{III} spectra as against only one sharp resonance B' in L_{II} spectrum (Fig.11). They have calculated the dipole transition intensities and the unoccupied valence levels and showed that there are two allowed p-->d transitions for the L_{III} edge and only one for L_{II} edge as experimentally found (Fig.12).
2. A spectacular example of application of EXAFS is provided by the work of Greaves and coworkers on osmium carbonyl clusters(ref.28) where identification of non-bonded metal-metal relationship is of prime importance in establishing the metal cluster skeleton. Three such separations in the decanuclear an ion $[Os_{10}C(CO)_{24}]^{2-}$ as seen by X-ray diffraction are clearly marked in the Fourier transform of the experimental and planewave spectra of Os L_{III}-edge EXAFS of $[P\,Rh_3)_3]\,N_2[\,Os_{10}C(CO)_{24}]$ (Fig.13).
3. Cramer and coworkers have reported a very interesting study of dynamic John-Teller distortions in $[Cu(1,2\text{-di amino ethane})_3][SO_4]$ by EXAFS which on account of lifetime ca10^{-10} sec) can give copper-ligand distances relating to the underlying static stereochemistry where X-ray crystallogrphic data would relate only to weighted thermal population of the various component structures. In(Fig.14) the EXAFS of the said compound shows no significant change in the

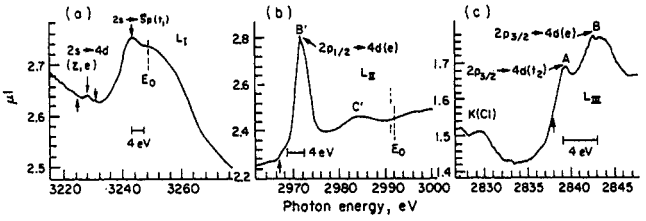

Fig. 11. Edge reion of $Ru(NH_3)_6Cl_3$: (a) Ru L_I, (b) Ru L_{II} and (c) Ru L_{III}; A, B, and B' are transitions to the 4d final states (ref. 27).

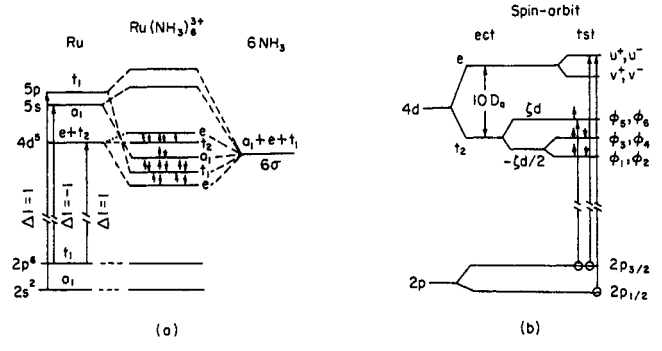

Fig. 12. (a) Simplified molecular orbital diagram of $Ru(NH_3)_6^{3+}$; according to O symmetry. (b) Energy diagram of the d-orbitals of $Ru(NH_3)_6^{3+}$; spin-orbit and tetragonal distortion are included. The spin-orbit wave functions ϕ_1 to ϕ_6 and u and v are in terms of the octahedral basis set and spin-functions. The three allowed 2p-->4d transitions are shown with arrows(ref. 27).

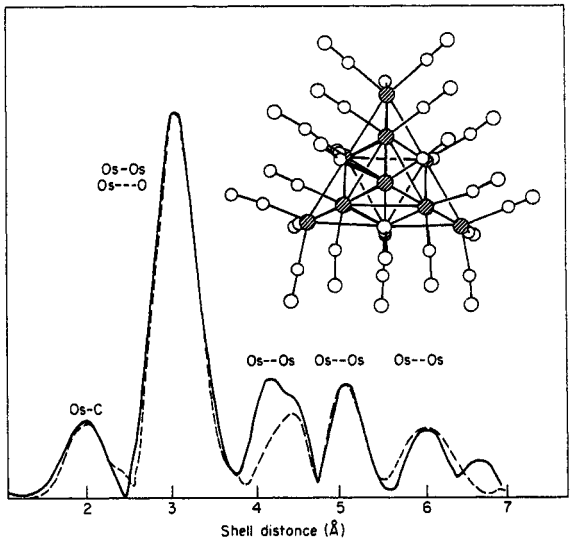

Fig. 13. Fourier transform of the experimental (————) and plane-wave (-------) spectra of the Os L_{III}-edge EXAFS of $[(PPh_3)_2N]_2[Os_{10}C(CO)_{24}]$. Crystal structure is also shown (ref. 28).

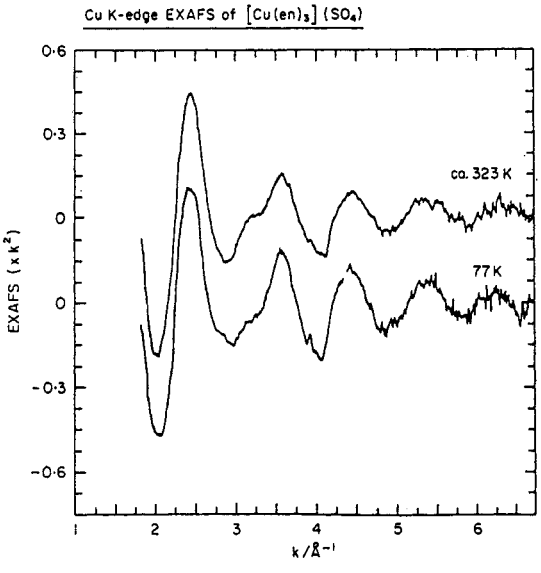

Fig. 14. Cu K-edge EXAFS of $[Cu(en)_3](SO_4)$ (ref. 29).

radial distribution about the copper on cooling from ca 300° to 77°K and the EXAFS is constant with six nitrogen atoms split into two shells at 2.04 and is 2.30Å whereas the diffraction measurement at room temperature indicated only one Cu-N distance of 2.15Å (ref.29) as against two C-N distances of 2.06 and 2.22Å at 120K. With more and more refinement in theory and more sophisticated instrumentation use is also being made of X-ray spectroscopy for surface studies(S EXAFS) and properties of alloys and catalysis.

REFERENCES

1. U.C. Srivastava and H.L. Nigam, Coord. Chem. Revs. 9,275 (1972-73).
2. H.L. Nigam, Proc. LXVIII Session Ind. Sci. Cong. Pt.II, Section IV, Varanasi, 1981.
3. H.L. Nigam, Proc. LII Session Natl. Acad. Sci India, Bhavnagar, 1982.
4. D.E. Sayers, E.A. Stern and F.W. Lyttle, Phys. Rev. Letters, 27, 1204 (1971).
5. C.A. Ashley and S. Doniach, Phys.Rev., B11, 1279 (1975).
6. P.A. Lee and J.B. Pendry, Phys. Rev., B11, 2795 (1975).
7. B.K. Teo and P.A. Lee, J. Am. Chem. Soc., 101, 2815 (1979).
8. A. Bianconi, XANES and their application to local structure determination, Daresbury Lab. Report DL/SCI/R17E.
9. C.R. Natoli,EXAFS and Near Edge Structure (Proc. Intl. Conf.Frascati-Italy, 1982), Eds. A. Bianconi, L. Incoccia and S. Stipcich, Berlin-Hiedelberg 1983, p. 43.
10. F.W. Kutzler, C.R. Natoli, D.K. Misemer, S. Doniach and K.O. Hodgson, J. Chem. Phys., 73, 3274 (1981).
11. S.P. Cramer and K.O. Hodgson, Prog. Inorg. Chem., 25, 1 (1979).
12. S.P. Cramer, K.O. Hodgson, W.O. Gillum and L.E. Mortenson, J. Am. Soc., 100, 3398 (1978).
13. H.L. Nigam, V. Krishna and J. Prasad, Inorg. Chim. Acta, 20, 193 (1976); H.L. Nigam, V. Krishna and U.C. Srivastava, Ind. J. Pure Appld. Phys., 832 (1976).
14. B.M. Kincaid and P. Eisenberger, Phys. Rev. Letters, 34, 1361 (1975).
15. "Synchrotron Radiation Reseach", Eds. H.Winick and S. Doniach,(Plenum Press New York, 1980).
16. R.H. Holm, T.E. Wolf, J.M. Berg, C. Warrick and K.O. Hodgson, J. Am. Chem. Soc., 100, 4632 (1978).
17. B.K. Teo, J. Am. Chem. Soc., 103, 3990 (1981).
18. B.K. Teo, EXAFS and Near Edge Structure (Proc. Intl. Conf. Frascati-Italy, 1982), Eds. A. Bianconi, L. Incoccia and S. Stipcich,Springer-Verlag Berlin- Hiedelberg 1983, p. 11.
19. J.B. Pendry, EXAFS and Near Edge Structure (Proc. Intl. Conf.Frascati-Italy, 1982), Eds. A. Bianconi, L. Incoccia and S. Sticich, Springer-Verlag Berlin- Hiedelberg 1983, p. 4.
20. A. Bianconi, S. Doniach and D. Lublin, Chem. Phys. Letters, 59, 121 (1978).
21. A. Bianconi, Appln. of Surface Sci., 6, 392 (1980).
22. A. Bianconi, EXAFS for Inorganic Systems, Eds. C.D. Garner and S.S. Hasnain, Daresbury Laboratory SERC DL/SCI/R17 (1981) p. 13.
23. P.J. Durham, J.B. Pendry and C.H. Hodges, Solid State Commn., 38, 159(1981).
24. A. Bianconi, EXAFS and Near Edge Structure (Proc. Intl. Conf. Frascati-Italy, 1982), Eds. A. Bianconi, L. Incoccia and S. Stipcich, Springer-Verlag Berlin-Hiedelberg 1983, p. 118.
25. P.J. Durham, EXAFS and Near Edge Structure (Proc. Intl. Conf. Frascati-Italy, 1982), Eds. A Bianconi, L. Incoccia and S. Sticich, Springer-Verlag Berlin-Hiedelberg 1983, p. 37.
26. A. Bianconi, M. Dell'Ariccia, A. Gargano and C.R. Natoli, EXAFS and Near Edge Structure (Proc. Intl. Conf. Frascati-Italy, 1982), Eds. A Bianconi, L. Incoccia and S. Sticich, Springer-Verlag Berlin-Hiedelberg 1983, p. 57.
27. T.K. Sham and B.S. Brunschwig, EXAFS and Near Edge Structure (Proc. Intl. Conf. Frascati-Italy, 1982), Eds. A Bianconi, L. Incoccia and S.Sticich, Springer-Verlag Berlin-Hiedelberg 1983, p. 168.
28. S.L. Cook, J. Evans, B.F.G. Johnson, J. Lewis, P.R. Raithby, R.B. Moyes, P.B. Wells, P. Worthington and J.N. Greaves, "EXAFS Studies on Transition Metal Clusters", Synchrotron Radiation (Appendix to the Daresbury Annual Report 1982-83), p. 83.
29. I. Ross, C.D. Garner, B.J. Hathaway and G.P. Diakun,"EXAFS Observations of Copper(II) Complexes Undergoing Dynamic Jahn-Teller Distortions", Synchrotron Radiation (Appendix to the Daresbury Annual Report 1982-83), p. 113.